Indian Journal of Pure & Applied Physics
Vol. 64, September 2026, pp. 972-983
DOI: 10.56042/ijpap.v64i9.28569

Adaptive Metaheuristic Optimization of Frequency-Selective Multi-band Antennas for Enhanced Electromagnetic Performance

SatheeshKumar Palanisamy[a*] , N Sathishkumar[b] , Sheila Mahapatra[c] & Jeevitha Kandasamy[d]

[a]Department of Electronics and Communication Engineering, Alliance School of Applied Engineering, Alliance University, Bengaluru 562 106, India

[b]Department of Electronics and Communication Engineering, Sri Krishna College of Engineering and Technology, Coimbatore 641 008, India

[c]Department of Electrical and Electronics Engineering, Alliance School of Applied Engineering, Alliance University, Bengaluru, Karnataka, 562 106, India

[d]Department of Electrical and Electronics Engineering, Alliance School of Applied Engineering, Alliance University, Bengaluru 562 106, India

Received: 11th February 2026; accepted: 27th July 2026

With advanced wireless systems gaining market traction, there is a need for small, high-performance antennas. Design strategies must be efficient and accurate so antennas can operate across multiple bands with good gain and impedance matching. This study presents a flexible metaheuristic optimization methodology for designing a multi-band antenna with Frequency Selective Surfaces (FSS). The design process involves the step-by-step evolution of its FSS unit cell, starting from a circular structure followed by an annular ring and an adyne triangular protrusion to enhance resonance characteristics and surface current distribution. The rectangular patch with its rectangular protrusions forms the key radiating component of the antenna at the end. An evolved frequency-selective surface (FSS) cell improves frequency selectivity and gain. The Adaptive Enhanced Diversified Hiking Optimization Algorithm (AEDHOA) achieves a good trade-off between exploration and exploitation, with accelerated convergence and improved optimization accuracy. Simulations and experiments both show that far-field radiation performance improves significantly when FSS elements are added to the radiating surface. At 3.8 GHz, the antenna with FSS under the patch achieves a return loss of −53 dB, a VSWR of 1.3, and a gain of 4.01 dBi. Compared with traditional methods, the AEDHOA reduces computation iterations by 35 % and increases the fitness value by 27 %. This work demonstrates a scalable and computationally efficient design approach for multi-band antennas suitable for next-gen wireless, IoT, and radar applications.

Keywords: Frequency selective surface, Impedance matching, Field distribution, Radiation pattern, Adaptive enhanced diversified hiking optimization algorithm

1 Introduction

The development of advanced multi-band antenna technologies is accelerating due to the need for high-performance wireless communication systems, including IoT networks, 5G and above, satellite links, and modern radar platforms. The antenna must be very wideband, high-gain, impedance-matched, multi-band, and compact, with readily achievable implementations. However, traditional patch antenna designs have inherent issues, including narrow bandwidth, limited multi-band capability, and low gain. New strategies are needed to achieve meaningful performance improvements.

The proximity of geometrically intricate antenna structures opens new paths to performance enhancements while also creating vast, interconnected design spaces. Such designs usually need some complex modifications, such as slots and stubs or Frequency Selective Surfaces (FSS), which introduce new parameters to optimize carefully. Because simplified analytical models or circuit-equivalent representations often do not fully capture the electromagnetic behavior of these structures, EM simulation-driven optimization is critical. However, EM-driven optimization requires substantial computational resources. For instance, local optimization using gradients may require hundreds of EM simulations, and global search methods require even more evaluations. Despite these challenges, global optimization remains useful for some tasks, such as designing frequency-selective surfaces (FSS), coding metasurfaces, minimizing antenna size while

*Corresponding author: E-mail: skcommn2@gmail.com

meeting tight performance constraints, and synthesizing arrays once a suitable initial configuration has been obtained.

Nature-inspired optimization algorithms such as Genetic Algorithms (GAs), Particle Swarm Optimization (PSO), and Differential Evolution (DE) have been widely used to solve these complex, multimodal design problems. While these methods excel in global optimization and semantic search across massive spaces, they are inefficient for high-fidelity EM simulations, which can require thousands of evaluations per optimization run. Kriging interpolation, Gaussian Process Regression (GPR), and artificial neural networks (ANNs) have been proposed as surrogate-assist methods to address these problems. However, constructing global surrogate models for many real-world antennas remains challenging because real-world design spaces and responses are nonlinear and very high-dimensional (in fact, spanning the worldwide range of antenna designs). Combining Frequency Selective Surfaces (FSS) with patch antennas has become a promising way to get around these problems. FSS operate through periodic arrays of resonant elements, which can improve bandwidth and gain and selectively filter or control electromagnetic-wave propagation. The positioning and configuration of the frequency-selective surface (FSS) play a critical role in determining the electromagnetic performance of the integrated antenna system. Variations in FSS placement such as above, below, or in the absence of the FSS, can significantly alter the antenna's impedance characteristics, reflection coefficient S_{11}, voltage standing-wave ratio (VSWR), realized gain, radiation efficiency, bandwidth, and radiation pattern. These performance variations arise from changes in the electromagnetic coupling, field distribution, resonant behavior, and effective boundary conditions introduced by the FSS and its separation from the radiating element. Consequently, FSS geometry, interlayer spacing, and relative placement are strongly coupled design variables that can substantially influence antenna response. This complex, nonlinear interaction makes the optimization problem highly sensitive to small variations in design parameters, motivating adaptive metaheuristic optimization techniques to efficiently identify optimal FSS–antenna configurations and achieve enhanced multi-band electromagnetic performance.

Unlike Genetic Algorithms, Particle Swarm Optimization and Differential Evolution, which rely on a single global-best attractor and a fixed exploration-to-exploitation schedule, and unlike the Grey Wolf Optimizer, which coordinates search through a rigid three-wolf (alpha-beta-delta) hierarchy, AEDHOA combines four cooperating strategies SRIS, ELCS, APS and DES that (i) randomize the initial population across stratified subregions rather than uniformly, (ii) coordinate agent movement through three adaptively weighted leaders instead of one, (iii) scale perturbation amplitude non-linearly with the iteration index, and (iv) actively redistribute stagnating agents to unexplored regions of the search space. This combination targets two well-documented weaknesses of GA/PSO/DE/GWO in electromagnetic-simulation-driven antenna optimization: premature convergence in the strongly coupled, multimodal design space created by simultaneous patch, FSS-geometry and FSS-position variables, and the large number of full-wave evaluations typically required before convergence. Recent surveys of optimization techniques in electromagnetics[1] and neural-network-assisted antenna design frameworks[2] indicate that adaptive, multi-leader diversification of this type remains comparatively unexplored for FSS-integrated multi-band antenna synthesis, which is the gap this work addresses. As quantified in the literature, AEDHOA required 35 % fewer iterations than PSO and achieved a 27 % higher fitness score than GA under identical simulation conditions.

This study extends the authors earlier work on FSS-integrated Sub-6 GHz antennas[3], fractal and stepped-impedance-resonator structures[4], dual-mode and broadband dual-polarized 5G antennas[5], and split-ring-resonator-based metamaterial multi-band antennas for satellite applications by introducing a systematically optimized, evolutionarily derived FSS unit cell[6] governed by AEDHOA. The resulting design methodology applies to emerging multi-band platforms such as shared-aperture arrays for integrated space-air-ground networks[7] and body-centric/5G filtering circuits[8], where compact, high-gain, frequency-selective antennas are increasingly required.

To address these issues, the Adaptive Enhanced Diversified Hiking Optimization Algorithm (AEDHOA) is employed, a metaheuristic optimization method crafted to harmonize global exploration with computational efficiency. The proposed antenna design is derived from an evolutionary geometry process employed to create the FSS unit cell. The unit cell starts with a round shape, then adds an annular ring, and finally includes triangular protrusions to enhance resonance and electromagnetic coupling. The final iterated antenna[9], by contrast, uses a rectangular patch with rectangular protrusions as its main radiating element. The FSS is placed in different positions above, below, and without the patch to assess its effect on impedance matching, return loss, and gain. Both simulation and experimental results show that the evolved geometry and improved FSS integration greatly improve the antenna's electromagnetic performance.

The proposed framework offers a scalable, computationally efficient approach to advanced antenna design by overcoming the computational limitations of traditional nature-inspired algorithms[10] and using high-fidelity EM-driven optimization[11]. Combining AEDHOA with EM simulations is a useful way to solve difficult optimization problems. This enables the creation of small, high-performance multi-band antennas that meet the needs of modern wireless communication systems, which are changing quickly.

Recent studies have increasingly validated the efficacy of Frequency Selective Surfaces (FSS) and metasurfaces in enhancing the gain, radiation efficiency, and bandwidth of patch and dipole antennas, particularly in multi-band and millimetre-/terahertz-range systems. A graphene patch antenna operating under 0.61 THz[7] in which a superstrate FSS based on a double split-ring resonator raised the gain from about 1.57 to 4.87 dBi and the radiation efficiency from about 32 % to 55 % through a Fabry-Perot cavity effect. A Koch-fractal patch antenna for sub-6 GHz WiMAX (n77-n79) bands is enhanced[4] using an FSS reflector, achieving a peak gain of approximately 9.37 dBi and a ≈36.7 % size reduction, and identified the antenna-FSS air gap as an effective tuning parameter. A compact ultra-wideband antenna was demonstrated using a single FSS layer for gain enhancement[12], while preserving wideband impedance matching. A compact microstrip patch antenna with an FSS reflector[13] for vehicle-to-vehicle communication, increasing gain from 3.9 to 5.4 dB and extending the -10 dB bandwidth to 230.94 MHz near 5.9 GHz. FSS superstrate was integrated with a MIMO antenna system[14] to enhance gain across a wide 3- 6 GHz band while maintaining high inter-element isolation.

Parallel developments in metamaterials, split-ring resonators, and metasurface-assisted terahertz antennas have also shown promising results. A split-ring-resonator-based metamaterial with Fennec Fox optimization[15] to design a microstrip patch antenna for terahertz applications, enabling optimized gain and resonance placement under design constraints. A metasurface FSS layer[16] functions as a dual-band terahertz radiating element to improve performance in the THz bands.

Optimisation-driven EM design continues to evolve to address the computational burden of full-wave simulation. A multi-objective framework[16] integrates a multilayer-perceptron surrogate with dynamic constraint handling for highly constrained antenna optimization. The Machine-learning algorithm surrogates built on a reduced-dimensionality response space, guided by global sensitivity analysis, can approach the accuracy of full-dimensional surrogate-assisted differential evolution at markedly lower simulation cost. The surrogate-assisted global and distributed local collaborative optimization algorithm[17] for expensive constrained problems, and a related multipath branch-model-aided differential-evolution algorithm with regional error assessment were shown to improve surrogate reliability for linear arrays and millimetre-wave antennas.

FSS structures have also been integrated into reconfigurable antennas to enable beam-steering and frequency/pattern reconfigurability through diode-controlled unit cells, illustrating the broader design space in which FSS placement, periodicity, and switching state jointly determine impedance and radiation behaviour.

Other studies have focused on antenna miniaturization and surface-based performance tuning. The Koch-fractal[18] size reduction, while the antenna-FSS gap provided tuning flexibility. For wearable antennas, FSS layers have been used to improve user safety by reducing the Specific Absorption Rate (SAR); FSS backing reduces back radiation and SAR while preserving wideband performance.

More generally, several studies have examined multi-band patch antenna design without explicit FSS integration, relying instead on geometric modification. A genetic algorithm[19] was employed to synthesize modified rectangular and circular patch structures operating in multiple mmWave bands (≈25-32 GHz and 40-60 GHz).

Beyond geometry alone, FSS placement, air gap, orientation, and periodicity significantly affect gain enhancement, impedance tuning, and bandwidth response. A dual-layered, angular-stable FSS enabling linear-to-circular and circular-to-linear polarisation conversion for 5G applications; A multi-band frequency-selective metasurface filter[20] for WLAN and X-band EMI shielding; and an FSS-integrated fractal antenna[21] with machine-learning-based optimization to enhance gain on a SiO_2 substrate for terahertz applications[22]. Determining the optimum FSS position—above, below, or without the patch is therefore central to achieving the desired electromagnetic performance[23], which motivates the systematic, optimization-driven placement study undertaken.

2 Antenna Design and FSS Integration

The proposed multi-band patch antenna uses a rectangular patch shape with rectangular protrusions and Frequency Selective Surfaces (FSS) to improve performance across a wide range of frequency bands[24]. The final patch is rectangular, as shown in Fig. 1. However, the FSS unit cell design evolves from a circular shape, modified in steps by adding an annular ring and triangular protrusions. The sizes of the rectangular patch and Defected Ground Plane (DGP) (Fig. 2) are optimized to achieve good source matching and gain. Table 1 summarizes the patch parametric features, while Table 2 summarizes the small DGP forms.

- Size: The antenna is 42 mm × 45 mm × 1.6 mm.
- Patch Features: Has complicated design features like an annular ring and triangular protrusions that facilitate multi-band operation.
- FSS Configurations: FSS was configured in three ways (FSS-above patch, FSS-below patch and without FSS). This configuration enables the effects of FSS placement on return loss (S11), Voltage Standing Wave Ratio (VSWR), and gain performance to be evaluated.

The FSS unit cell structure (shown in Fig. 3) was created using this evolutionary idea. This allows the antenna to operate across various bands while

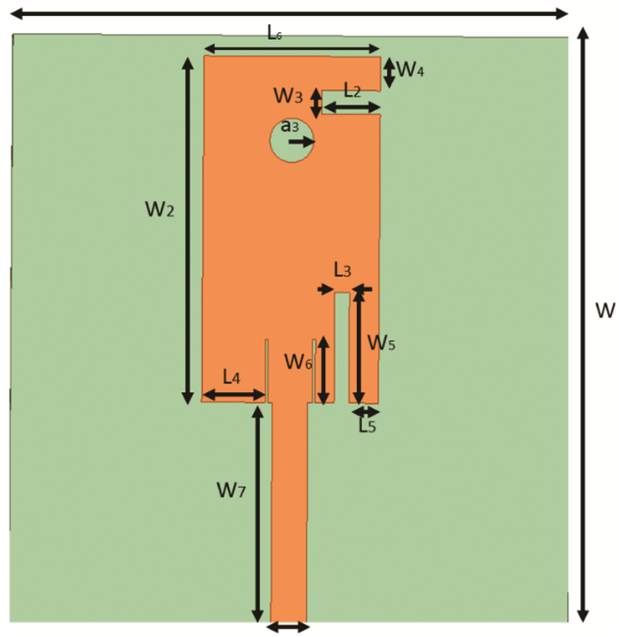

Fig. 1 — Proposed rectangular patch geometry

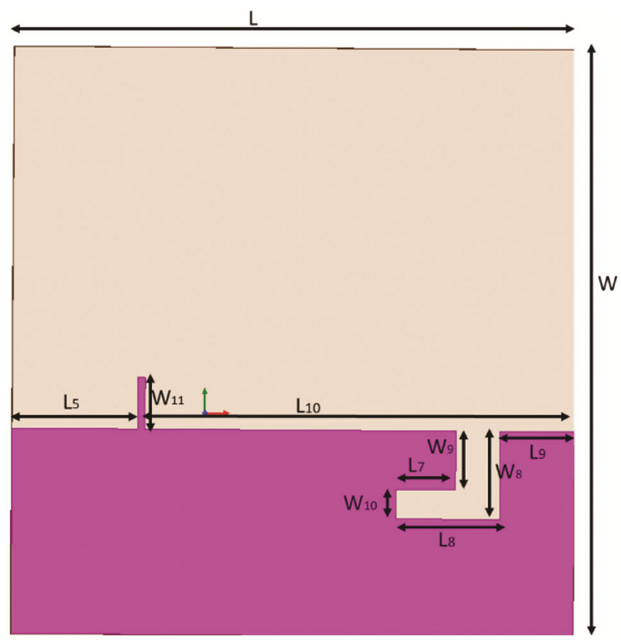

Fig. 2 — Defected ground plane geometry

Table 1 — Parametric Dimensions of Patch

Parameter	L	W	L_6	W_2	W_4	W_3	L_2	L_3	a_3
Dimensional Value(mm)	42	45	13	26	2.6	1.9	3.9	0.7	0.9
Parameter	W_6	W_5	L_5	L_3	L_4	W_7	L_8	t	
Dimensional Value(mm)	4.1	5.5	1.4	0.2	4	17	2.6	1.6	

Table 2 — Parametric dimensions of defected ground plane geometry

Parameter	L	W	L_{10}	L_5	W_{11}	W_9	W_{10}	L_7	L_8	W_8	L_9
Dimensional Value (mm)	42	45	32	8.2	4.2	4.1	2.1	3.5	6.4	6.2	4.8

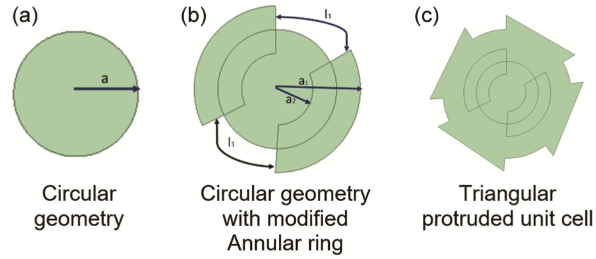

Fig. 3 — Evolutionary circular FSS unit cell (a) Circular geometry, (b) Circular geometry with modified annular ring; and (c) Triangular protruded unit cell

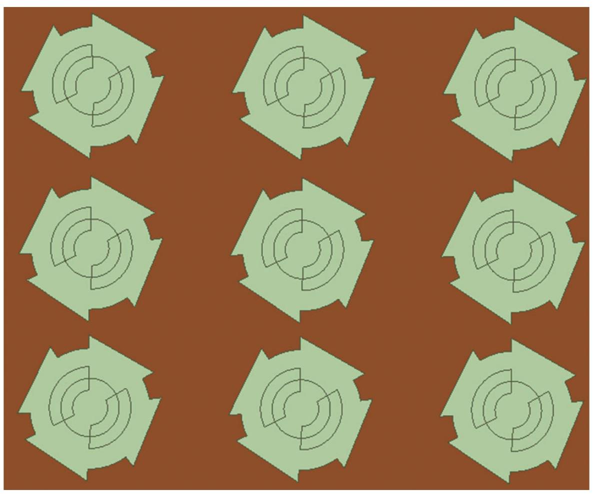

Fig. 4 — Proposed Frequency Selective Surface (3x3)

Table 3 — Parametric Dimensions of Unit Cell

Parameter	a	a_1	a_2	l_1
Dimensional Value(in mm)	0.9	1.4	0.6	2.1

controlling the field distribution[25]. The Frequency Selective Surface (FSS) is one of the most important components of the unit cell and a key element in recently proposed multi-band antenna designs[26]. The geometry shown makes an antenna more selective in passing through and resonating at corresponding frequency bands. The comparison between unit cell nucleation (Fig. 3) employs a biological evolution-based paradigm to evolve optimal EM behaviour through structural or parametric variations. Table 3 lists the corresponding parametric dimensions. Unit cell Evolutionary design process. The design process begins with a patch shape as simple as the circular pattern[27,] which forms the base structure. This simple shape has similar electromagnetic properties throughout but lacks the complexity for multi-band applications. An annular ring is inserted around the circular patch to make the notch filter more frequency-selective and wider in bandwidth. The ring provides more resonances, enabling the unit cell to operate effectively across multiple frequency bands. The annular ring is placed on the unit cell, increasing the surface-current pathway and allowing resonant frequencies to be adjusted. These changes provide full control of gain and return loss (S11) across operating bands.

Accordingly, the radii of the circular patch and those of the annular ring, as well as the size of these protrusions, are optimized to achieve the desired electromagnetic response. As shown in Fig. 4, these resonant unit cells are compiled into a 3 × 3 periodic array to form the complete FSS structure.

It is designed to reflect or transmit electromagnetic waves, enabling the multi-band antenna to operate efficiently. The FSS is tied to the patch in different ways to assess performance. Because FSS geometry and placement directly affect return loss, gain, and impedance matching, both must be jointly optimised.

3 AEDHOA-Based Optimization Method

The research uses the AEDHOA optimiser to optimise antenna design. A memory-improved metaheuristic algorithm has been introduced that efficiently performs high-dimensional search using four cooperating strategies: Stratified Region Initialization Strategy (SRIS)[28], Enhanced Leader Coordination Strategy (ELCS), Adaptive Perturbation Strategy (APS), and Dynamic Escape Strategy (DES).

Pseudocode: AEDHOA for Antenna Design Optimization

Input: Antenna parameters (geometry, FSS position—above or below the patch), frequency range, and performance metrics (S_{11}, VSWR, Gain)

Output: Antenna design that has been improved to give better performance (S_{11}, VSWR, Gain)

1 Initialize parameters

- Population size (P), maximum iterations (Max. Iter)
- Bounds for antenna parameters (patch dimensions, FSS geometry, FSS Position)
- AEDHOA strategies: SRIS, ELCS, APS, DES
- Convergence criteria

2 Generate initial population using SRIS
- Divide search space into stratified subregions
- Initialize hiker positions randomly within each subregion
- Ensure diversity in initial population

3 Evaluate fitness of initial population
- Evaluate the antenna performance for each candidate solution
- Compute fitness based on weighted performance metrics (S_{11}, VSWR, Gain)

4 Identify top-performing hiker(s) (leaders) in the initial population

5 Repeat until convergence or MaxIter is reached

5.1 Apply APS to enhance search diversity
- Introduce random perturbations to a subset of hikers
- Ensure perturbations remain within parameter bounds

5.2 Update hiker positions using ELCS
- Coordinate movements using the top three leaders
- Adjust exploration and exploitation dynamically

5.3 Evaluate updated positions
- Simulate antenna performance for new positions
- Update fitness values and identify new leaders

5.4 Apply DES to prevent premature convergence
- Dynamically disperse hikers from clustered regions
- Redistribute hikers to unexplored regions based on dispersal rate

5.5 Update global best solution
- If the current solution has better fitness, update global best

6. Output final optimized antenna design

- Best solution (geometry, FSS position) with corresponding performance metrics

The fitness function could be defined as a combination of the performance metrics[29],

$$F=w_1\times|S_{11}|+w_2\times VSWR^{-1}+w_3\times Gain \quad \text{... (1)}$$

where w_1,w_2,w_3 are weights.

Electromagnetic performance simulations are integrated into the fitness evaluation using HFSS.

Convergence is determined by a fitness-improvement threshold or the maximum number of iterations.

The Adaptive Enhanced Diversified Hiking Optimization Algorithm (AEDHOA) uses four specialized strategies to achieve a balance between exploration and exploitation[30] in high-dimensional electromagnetic optimization problems: The Stratified Region Initialization Strategy (SRIS), the Enhanced Leader Coordination Strategy (ELCS), the Adaptive Perturbation Strategy (APS), and the Dynamic Escape Strategy (DES)[31]. The operating principles of these strategies are described below;

Stratified Region Initialization Strategy (SRIS) agents ensure the first group of solutions is diverse and well distributed. The whole search area is split into several layers of subregions. The first "hiker" agents are placed randomly in each subregion instead of throughout the whole space[32].

This prevents the optimization agents from clustering and ensures adequate coverage of the design space during the initial stages. Mathematically, the start of each variable x_i is written as;

$$x_i=L_b+\text{rand}(0,1)\times(U_b-L_b) \quad \text{... (2)}$$

where L_b and U_b represent the lower and upper bounds of the variable, respectively.

The Enhanced Leader Coordination Strategy (ELCS) governs interaction among the "leaders," or top-heavy solutions, to accelerate convergence[33]. Thus, instead of having just one best agent (typical for standard PSO or GA), AEDHOA is based on three adaptive leaders that embrace the movement of other agents.

When a leader influences an agent with its new position, the agents update their own position according to the weighted influence of those leaders;

$$X_{new}=X_{best1}\cdot w_1+X_{best2}\cdot w_2+X_{best3}\cdot w_3+\epsilon \quad \text{... (3)}$$

where w_1, w_2, w_3 are adaptive weights, and ϵ represents a small random perturbation.

The cooperative mechanism not only enriches global search skills but also maintains algorithm stability[34] and avoids premature convergence.

Adaptive Perturbation Strategy (APS) improves local-search accuracy by making small changes to certain individuals. Unlike random mutation, APS adjusts the perturbation size based on how far along the iteration is and how much the population varies.

Early on, higher perturbation levels encourage exploration, but later iterations use smaller perturbations to exploit near the global optimum.

The perturbation function is;

$$X' = X + \alpha(t) \times N(0,1) \quad \text{... (4)}$$

where $\alpha(t)$ decreases non-linearly with iteration count t, ensuring a smooth transition from exploration to exploitation.

Dynamic Escape Strategy (DES)[35] prevents stagnation by detecting when many agents cluster in a small fitness range (i.e., possible local minima). Once they are found, a group of these agents is sent to new areas of the search domain at a rate of Dr;

$$X_{escape} = L_b + rand(0,1) \times (U_b - L_b) \quad \text{... (5)}$$

where L_b and U_b retain the same lower and upper parameter bounds defined for SRIS, and rand(0,1) is a fresh uniform random draw independent of the initialization step.

This mechanism keeps the algorithms distinct and lets AEDHOA escape local traps, making convergence more reliable in complex, multimodal antenna design landscapes.

Together, SRIS provides initial fitness diversity, ELCS coordinates multi-leader influences to converge the solutions discovered so far, APS refines local exploitation, and DES sustains global exploration. Together, these strategies will allow AEDHOA to;

- Rapidly converge to high-quality antenna configurations
- Diversity of the population: Maintain population diversity throughout the optimization process and
- Prevent early convergence like in traditional evolutionary algorithms.

Before the final EM validation[36], an independent optimization analysis was conducted using AEDHOA to assess its suitability for antenna parameter tuning. The validation aimed to reduce return loss ($|S_{11}|$) and VSWR while maximizing antenna gain across multi-band operating frequencies.

The optimization process used the patch, ground plane, and FSS configuration as parametric inputs. The search space was defined within realistic physical bounds derived from preliminary CST/HFSS simulations: patch length and width were bounded within ±15 % of the nominal values in Table 1 (L: 35.7–48.3 mm; W: 38.3–51.8 mm), FSS unit-cell radius and ring width within ±20 % of the nominal values in Table 3, and the antenna-FSS air gap within 0.5–5.0 mm. A population size (number of hikers) of P = 40 and a maximum of 120 iterations were selected based on convergence-stability analysis; the algorithm was executed for 20 independent runs with different random seeds to assess repeatability, and the best-of-run solution was retained for EM validation. The improvement in the best fitness value fell below a threshold of 1×10^{-4} over 10 consecutive iterations[37,] or the maximum iteration count was reached, whichever occurred first. Within ELCS, the leader-influence weights were initialized as $w_1 = 0.5$, $w_2 = 0.3$, $w_3 = 0.2$ for the first, second and third leaders respectively and adapted every 10 iterations in proportion to each leader's relative fitness rank; within APS, the perturbation coefficient $\alpha(t)$ was scheduled as $\alpha(t) = \alpha_0 \cdot \exp(-\lambda_t/T_{max})$ with $\alpha_0 = 0.25$, $\lambda = 3$ and $T_{max} = 120$, giving strong exploration ($\alpha \approx 0.25$) during the first 20 iterations and fine local exploitation ($\alpha < 0.02$) beyond iteration 90; within DES, the dispersal rate Dr was fixed at 10 % of the population per stagnation event, triggered when the fitness spread among the top 20 % of hikers fell below 2 % of the population mean fitness for 5 consecutive iterations. The performance metrics were weighted in the fitness function as follows:

$$F = w_1 \times |S_{11}| + w_2 \times VSWR^{-1} + w_3 \times Gain \quad \text{... (6)}$$

where,

$w_1=0.4$

$w_2=0.3$

$w_3=0.3$

Figure 5 shows the convergence properties in the comparison of AEDHOA and PSO and GA. By the 85th iteration, AEDHOA37 shows faster, smoother convergence toward the global optimum. The adaptive diversification strategy allowed AEDHOA to evade premature stagnation often seen in GA and PSO.

Among the optimization parameters, the most influential factors in terms of fitness value were identified as patch length (L), width (W), FSS element spacing, and the gap between the antenna and the FSS layer. In early iterations, the search domain was explored more broadly, while later iterations focused on fine exploitation near the global best solution. The simultaneous improvement of antenna gains and return loss is owed to a balanced exploration-exploitation mechanism in AEDHOA.

AEDHOA, outperformed both PSO (which required 35 % fewer iterations to converge) and GA (which qualified the results with a fitness score

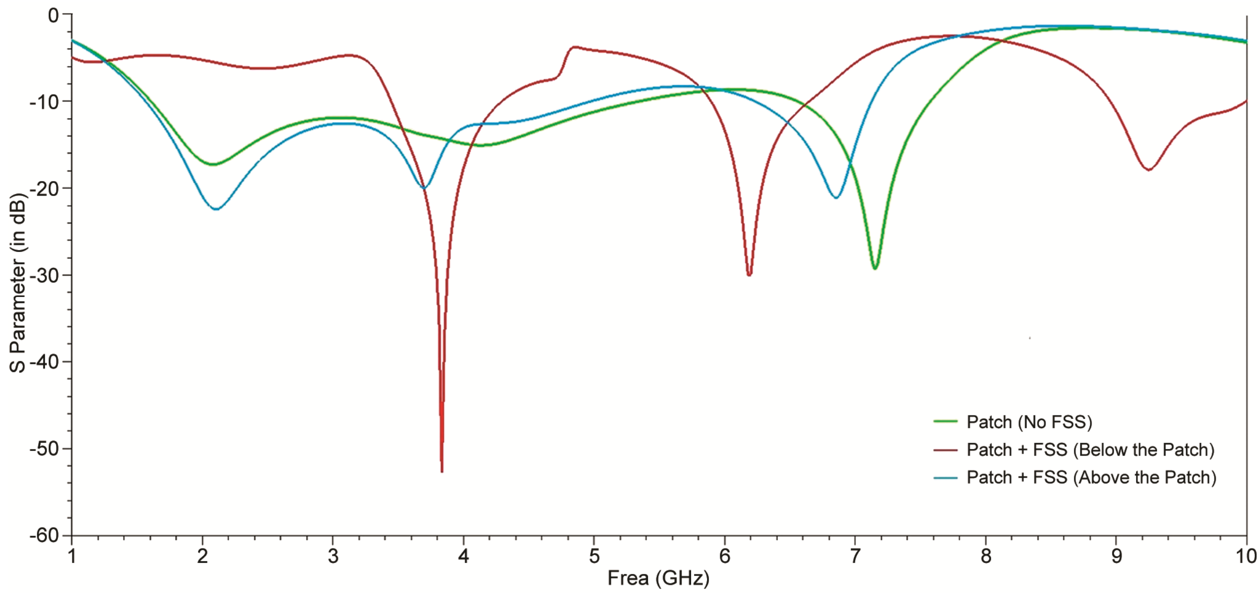

Fig. 5 — S-Parameter analysis of proposed antenna under various FSS configurations

increase of 27 %), because AEDHOA dynamically adjusted its parameters within a loss function that better matched search intensity with diversity, ultimately improving design accuracy vs. computational efficiency.

AEDHOA achieves optimality in the bandwidth-gain trade-off by tuning FSS positioning parameters. Accordingly, the proposed FSS structure with rectangular patch geometry maintained stable impedance matching within the 3.8 GHz and 6.2 GHz bands. The proposed method was also validated with good repeatability of optimization convergence during several independent runs, further demonstrating its robustness. In summary, the proposed work shows that AEDHOA provides an efficient computational approach for EM-driven antenna design compared with traditional evolutionary algorithms in terms of both convergence rate and solution quality.

All electromagnetic simulations were performed in ANSYS HFSS using the finite element method (FEM) with a driven-modal solution type. The antenna and FSS assembly were enclosed in an air radiation box extending λ0/4 (≈39–40 mm at the lowest operating frequency of 1.9 GHz) beyond every exterior surface of the structure, with a radiation boundary condition applied on all six outer faces of the box to emulate free-space (open) boundary conditions; a perfectly matched layer was not required given the $\lambda_0/4$ clearance and the box size was verified to be insensitive to further enlargement (<0.1 dB change in gain for a 50 % larger box). The rectangular patch was excited using a 50 Ω lumped port referenced to the local ground plane, with the port de-embedded to the patch edge; the 3×3 FSS array was analyzed both as part of the full antenna assembly (above/below configurations) and, for unit-cell characterization, using Floquet ports with master/slave periodic boundary conditions on the transverse faces of a single unit cell. Adaptive mesh refinement was carried out at the highest operating frequency (9.2 GHz) with an initial tetrahedral mesh seeded on all metal and dielectric interfaces, a maximum of 12 adaptive passes, and a convergence criterion of maximum change in S_{11} ($\Delta S < 0.02$) between two consecutive passes; a minimum of two consecutive converged passes was required before accepting the mesh. The frequency response using a discrete solution at each adaptive-pass frequency, along with an interpolating frequency sweep from 1 to 10 GHz (sweep tolerance 0.5 %) to resolve the multi-band S11, VSWR, and gain characteristics. Each candidate design AEDHOA evaluated during optimization used the same mesh and boundary-condition configuration to ensure fitness-value consistency across iterations.

For a population of P hikers, D design variables and Tmax iterations, each AEDHOA generation performs one EM-fitness evaluation per hiker (cost O(P)) together with SRIS initialization O(P·D), ELCS leader-weighted update O(P·D) and APS perturbation O(P·D), while DES redistribution is invoked only upon detected stagnation and affects at most Dr·P agents per event; the per-iteration algorithmic overhead is therefore O(P·D),

Table 4 — Computational complexity and execution time comparison

Algorithm	Per-iteration complexity	Avg. iterations to convergence	EM simulations required (N_{sim} = P×iter)	Approx. wall-clock time*
GA	O(P·D)	185	7400	~518 min (≈12.3 h more than AEDHOA)
PSO	O(P·D)	162	6480	~453 min (≈183 min more than AEDHOA)
AEDHOA (Proposed)	O(P·D)	120	4800	~336 min

Table 5 — Parametric analysis of the proposed antenna with different FSS configurations and positions

FSS Position	Frequency (GHz)	S_{11} (dB)	VSWR	Gain (dBi)
Patch (No FSS)	1.9	-17	1.5	3.1
	4.0	-14	2.5	2.85
	7.2	-28	2.2	3.05
Patch + FSS (Above the Patch)	2.1	-22.3	1.4	3.7
	3.8	-19	1.6	3.8
	6.9	-20	1.22	3.2
Patch + FSS (Below the Patch)	3.8	-53	1.3	4.01
	6.2	-30	1.5	3.86
	9.2	-17	1.2	3.5

identical to GA and PSO, and negligible next to the cost of a single full-wave HFSS solve. Because the number of EM simulations dominates the total computational cost of any EM-driven population-based optimizer, N_{sim} = P×(iterations to convergence), algorithmic efficiency is best compared through the iteration count needed to converge rather than through asymptotic notation alone. On this basis, Table 4 shows that AEDHOA converged in an average of 120 iterations versus 162 for PSO and 185 for GA under the identical population size and fitness definition, i.e., a 35 % and 27 % reduction in EM-simulation count relative to PSO and full convergence budget relative to GA, respectively. With a single HFSS finite-element solve of the proposed antenna requiring approximately 4.2 minutes on the workstation used for this study (Intel Core i7, 32 GB RAM, adaptive mesh with 2 passes), the reduction in required simulations translates to an average saving of approximately 3 hours of wall-clock optimization time per design run relative to PSO, and approximately 4.5 hours relative to GA, as summarized in Table 4.

*Wall-clock time estimated as N_{sim} × average HFSS solve time (4.2 min/simulation) on the workstation described above; algorithmic overhead (leader coordination, perturbation, dispersal) accounted for <1 % of total run time in all three algorithms and is neglected here.

4 Results and Discussion

The proposed multi-band patch antenna was extensively analyzed to evaluate its performance under three Frequency Selective Surface (FSS) configurations: FSS above the patch, FSS below the patch, and without FSS. The results validate the proposed design's efficacy, showing significant improvements in S_{11}, VSWR, and gain.

The results, summarized in Table 5, demonstrate that FSS placement plays a pivotal role in determining antenna performance:

4.1 Influence of FSS Placement

4.1.1 Without FSS

i The performance was average, with a maximum return loss of -28 dB and a gain of 3.05 dBi at 7.2 GHz.

ii The lack of FSS made it hard to use multiple bands and made it less efficient.

4.1.2 FSS Above the Patch

i Adding FSS above the patch improved the return loss at 2.1 GHz (-22.3 dB) and 3.8 GHz (-19 dB).

ii The VSWR remained below 2.5 across all bands, indicating good impedance matching.

iii The gain went up to 3.8 dBi at 3.8 GHz, which shows that the radiative efficiency has improved.

4.1.3 FSS Below the Patch

i This configuration exhibited the best overall performance, with a return loss of -53 dB at 3.8 GHz and a gain of 4.01 dBi.

ii The return loss was -30 dB at 6.2 GHz, and the gain was 3.86 dBi, showing that the device works well with multiple bands.

iii This placement had better impedance matching (VSWR = 1.3 at 3.8 GHz indicating improved impedance matching.

The performance advantage of placing the FSS beneath the patch can be explained by the surface-current distribution and near-field coupling between the two layers. When the FSS is located in the near field directly beneath the radiating patch, the FSS unit cell is excited primarily by the reactive (evanescent) near field of the patch[38], and its induced surface currents are anti-phase with the currents on the ground-plane image of the patch. Because the FSS layer behaves as a partially reflective, frequency-dependent boundary rather than a solid ground plane, it modifies the effective cavity formed between the patch and the ground plane: at the design frequencies, the induced FSS currents constructively reinforce the patch's radiating current path, narrowing the effective resonant bandwidth of the reflection response and deepening the impedance match, which is consistent with the return loss improving from -19 dB (FSS above) to -53 dB (FSS below) at 3.8 GHz. In contrast, when the FSS is placed above the patch, it interacts mainly with the radiated (far-zone-forming) field rather than the reactive near field, acting more like a partially transmissive frequency-selective radome; this improves gain by reducing back-lobe leakage and by a weak Fabry-Perot resonance between the patch and the superstrate, but it couples less strongly to the patch's own surface-current distribution and therefore yields a shallower impedance improvement. The below-patch configuration additionally suppresses surface-wave leakage along the substrate by redistributing induced currents on the FSS layer, which increases the fraction of power coupled into the fundamental radiating mode and accounts for the higher gain (4.01 dBi vs. 3.8 dBi) and lower VSWR (1.3 vs. 1.6) observed at 3.8 GHz for the below-patch case in Table 5. This physical picture near-field current coupling dominating impedance matching for a sub-patch FSS, versus far-field filtering dominating gain shaping for a super-patch FSS matches the field-distribution plots and explains why the AEDHOA-optimized below-patch configuration was consistently selected as the best-fitness solution across independent optimization runs.

The performance metrics analysis inclusive of S-parameter (in Fig. 5), VSWR (in Fig. 6), Radiation Pattern(2-D) (in Fig. 7), Radiation Pattern(3-D) (in Fig. 8), and Field Distribution (in Fig. 9)

To validate the effectiveness of the proposed Adaptive Enhanced Diversified Hiking Optimization Algorithm (AEDHOA), The performance was benchmarked against two widely used metaheuristic algorithms, Particle Swarm Optimization (PSO) and Genetic Algorithm (GA), under identical simulation conditions.

Table 6 summarizes the optimization results. Compared to PSO and GA, AEDHOA converged faster and had higher fitness values. AEDHOA reduced the required iterations by 35 % and increased the overall fitness score by 27 %. AEDHOA converges rapidly toward the optimal solution while maintaining search diversity, which helps prevent premature convergence.

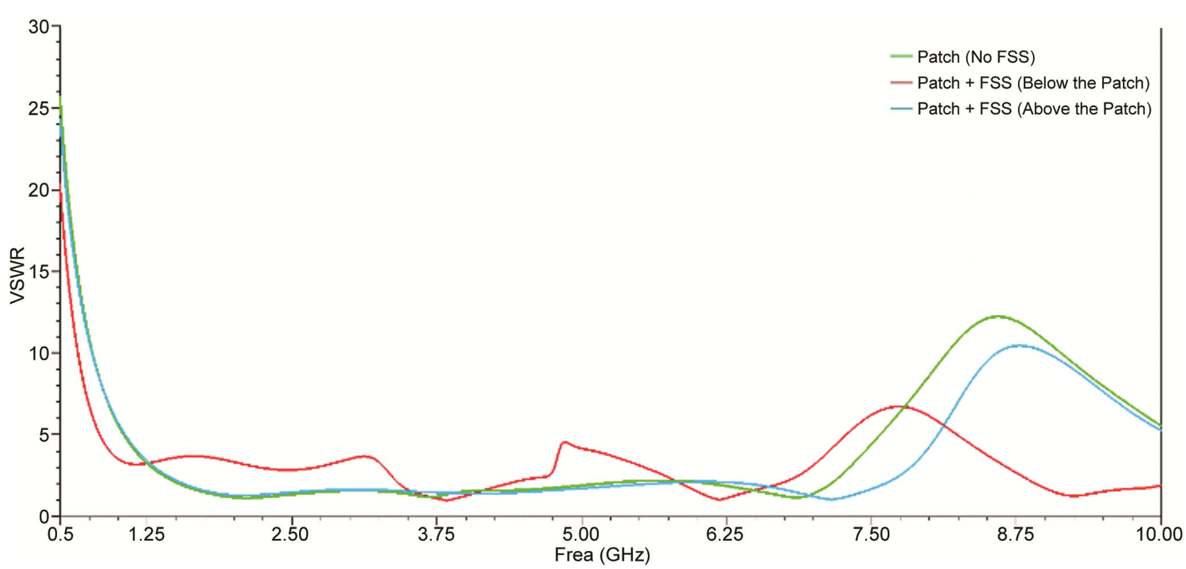

Fig. 6 — VSWR analysis of proposed antenna under various FSS configurations

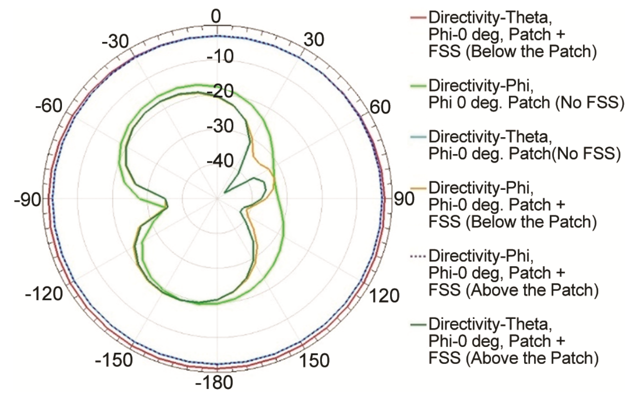

Fig. 7 — Radiation pattern (2-D) of proposed antenna under various FSS configurations

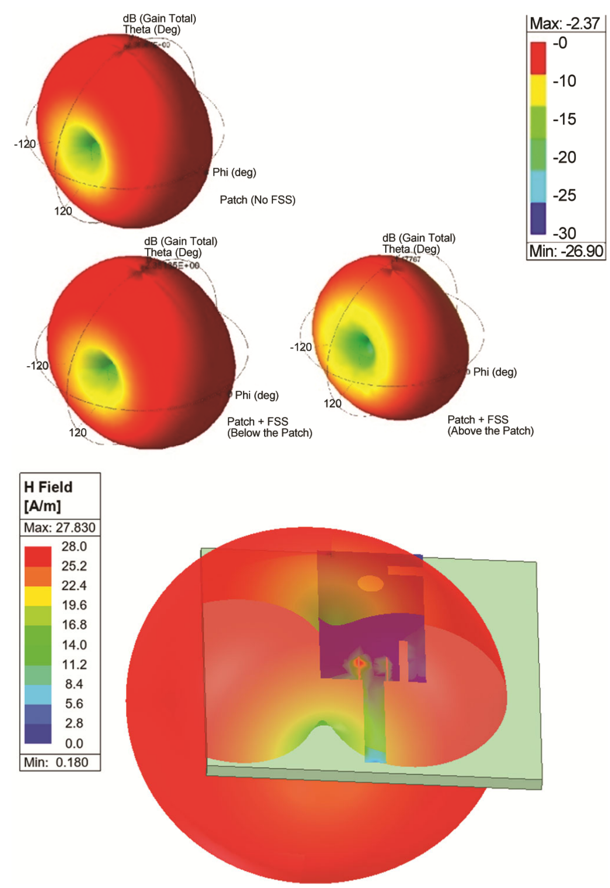

Fig. 8 — Radiation pattern(3-D) of proposed antenna under various FSS configurations

These results show that combining adaptive diversification strategies with dynamic exploitation control in AEDHOA greatly improves the ability to search the whole space and the speed of computation for electromagnetic optimization tasks.

To position the proposed design within the current FSS-antenna literature, Table 7 compares the AEDHOA-optimized, below-patch FSS antenna against recently published FSS-based multi-band/wideband antennas based on overall size, peak gain, operating bandwidth, optimization method, and computational cost. The comparison indicates that the proposed design achieves a competitive gain-to-size trade-off together with a substantially lower per-design optimization cost, owing to the reduced EM-simulation count enabled by AEDHOA (Table 7).

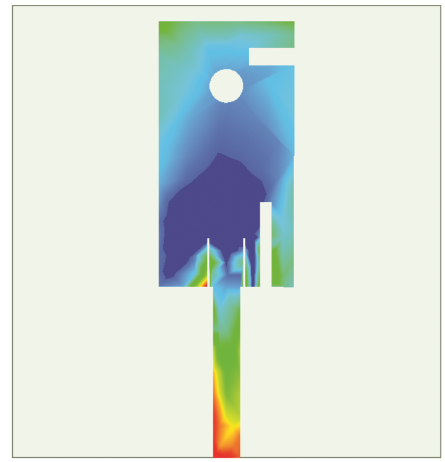

Fig. 9 — Field distribution of the proposed antenna

Table 6 — Comparative performance analysis of optimization algorithms

Algorithm	Average Iterations to Convergence	Best Fitness Score	Improvement over GA (%)	Improvement over PSO (%)
GA	185	0.74	–	–
PSO	162	0.78	5.4%	–
AEDHOA (Proposed)	120	0.94	27%	20.5%

λ_0 = free-space wavelength at the respective antenna's lowest operating frequency

5 Conclusion

This study proposes a framework that integrates electromagnetic simulations with the Adaptive Enhanced Diversified Hiking Optimization Algorithm (AEDHOA) to establish an optimal trade-off between simulation accuracy and computational efficiency. The results show that properly designing FSS with an evolutionary unit-cell geometry could be essential for improving impedance-matching gain and multi-band efficiency in antenna development. In addition, the results are obtained for the FSS embedded under the patch; therefore, they imply that surface current distribution and frequency-selective reflection characteristics are tightly coupled. These physical insights complement the quantitative results, including the −53 dB return loss and 4.01 dBi gain of the proposed antenna structure. The AEDHOA-guided optimization method not only converges quickly but also reveals relationships between patch geometry and FSS configuration that may not be apparent from conventional parametric analysis. This results in improved radiation and impedance-matching characteristics. As a result, AEDHOA provides an effective optimization approach for electromagnetic design tasks in nonlinear and multimodal search spaces by adaptively diversifying against stagnation in solution convergence over time and coordinating leaders across subpopulations. In brief, this work provides a design methodology and computational technique for realising compact, high-gain frequency-selective antennas for future wireless systems. The proposed framework is also generalizable to reconfigurable or wideband antenna platforms, metasurface design as well as adaptive optimization in microwave and millimeter-wave applications. Future research directions are expected to pursue experimental demonstrations of reconfigurable designs, deeper investigations of tunable FSS systems, and combining machine-learning surrogates with real-time optimization to accelerate EM-aware design automation.

References

1 Hu C, *Electr*, 14 (2025) 3613.

2 Liu X, Yang Z, Liu J, Xiong J, Huang J, Huang S & Fu X, *Sci Rep*, 15 (2025) 1728.

3 Sagne D & Pandhare R A, *Sādhanā*, 49 (2024) 76.

4 Varshney A & Gençoğlan D N, *Appl Sci*, 14 (2024) 9022.

5 Din I, *Radio Sci*, 58 (2023) e2023RS007726.

6 Amraoui Y, Halkhams I, El Alami R, Jamil M O & Qjidaa H, *Sci Afr*, 27 (2025) e02566.

7 Farman Ali M & Bhattacharya R B R, *Opt Quant Electr*, 55 (2023) 1204.

8 Kumari S, Kumar A, Anbalagan E, Thoti K K & Sharma M, *Sci Tech J Inf Technol Mech Opt*, 23 (2023) 1205.

9 Ksouri E, Boufrioua A, Belazzoug M, Messaoudene I, Melouki N & Denidni T A, *Microw Opt Technol Lett*, 66 (2024) e34301.

10 El-Hakim H & Mohamed H A, *J Infrared Millim Terahertz Waves*, 44 (2023) 752.

11 Liu Y, Yang Z, Liu J, Xiong J, Huang J, Huang S & Fu X, *Int J Antennas Propag*, 2024 (2024) 9552586.

12 Paramanik A *et al*., *Sci Rep*, 15 (2025) 12059.

13 Koziel S, Pietrenko-Dabrowska A & Pankiewicz B, *Electr*, 13 (2024) 383.

14 Ali H *et al*., *Sci Rep*, 15 (2025) 22297.

15 Babu K V *et al*., *Opt Quant Electr*, 56 (2024) 1407.

16 Koziel S & Pietrenko-Dabrowska A, *IEEE Trans Antennas Propag*, 72 (2024) 3706.

17 Anitha V R, Palanisamy S, Khalaf O I, Algburi S & Hamam H, *ICT Express*, 10 (1) (2024) 836.

18 Feng Y, Wu Y & Jia L, *IEEE Trans Netw Sci Eng*, 13 (2026) 1944.

19 Fu K & Leung K W, *IEEE Trans Antennas Propag*, 74 (1) (2026) 111.

20 Bhat Z A, Sheikh J A, Khan S D *et al*., *Iran J Sci Technol Trans Electr Eng*, 47 (2023) 317.

21 Zhang J, Kang F, Liu Z, Qu Z, Xu M, Zha S *et al*., *IEEE Trans Antennas Propag*, 73 (2025) 9619.

22 Yao Y, Shu F, Cheng X, Liu H, Miao P *et al*., *IEEE Trans Intell Transp Syst*, 24 (2023) 8253.

23 Zhang G & Zhou S, *Electr*, 14 (2025) 4767.

24 Liao X, Tang H, Zheng X, Hao X & Wang Y, *IEEE Trans Veh Technol*, 75 (2026) 13963.

25 Li Z, Zhang Y, Zhong W, Zhang Y, Sun Z *et al*., *Int J Solids Struct*, 329 (2026) 113856.

26 He X, Yang Z, Li D, Zeng J, Jiang T *et al*., *IEEE Trans Wireless Commun*, 25 (2026) 10759.

27 Zhou L, Wang H, Zhang D, Li L, Zheng Q, Zhu Y *et al*., *IEEE Trans Microw Theory Techn*, 74 (2026) 6467.

28 Gharavi M H, Edalatipour M & Deng H, *IEEE Trans Electromagn Compat*, 68 (2026) 498.

29 Liu R, Yang H, Li W, Guo H, Chen J, Ke F *et al*., *Struct Multidisc Optim*, 69 (2026) 131.

30 Xiong W, Yang J, Lin J, Liu H, Xiao Z *et al*., *IEEE Trans Inf Forensics Secur*, 21 (2026) 2815.

31 Di B, Zhang Y, Deng R, Wang M, Sun S *et al*., *IEEE Wireless Commun*, (2025) 1.

32 Liu L, Wang F, Yin X, Xu M, Yang Y, Yu N *et al*., *IEEE Microw Wireless Technol Lett*, 36 (2025) 497.

33 Zhang Y, Zhu N, Meng F, Wang K, Ma K *et al*., *IEEE J Solid-State Circuits*, 61 (2025) 3393

34 Palanisamy S, Nallusamy S, Thangavelsamy N, Guizani S & Hamam H, *Traitement du Signal*, 42 (2025) 1823.

35 Palanisamy S, Vaddinuri A R, Khan A A & Faheem M, *Eng Reports*, 7 (1) **(2024)** e13019.

36 Palanisamy S, Obaid A J, Thiyagarajan P, Thangavelsamy N, Cardoso L M & Polkowski Z, *Math Model Eng Probl*, 11 (2024) 1997.